

Effect of Nickel Concentration on Bias Reliability and Thermal Stability of Thin-Film Transistors Fabricated by Ni-Metal-Induced Crystallization

This content has been downloaded from IOPscience. Please scroll down to see the full text.

2012 Jpn. J. Appl. Phys. 51 011301

(<http://iopscience.iop.org/1347-4065/51/1R/011301>)

View [the table of contents for this issue](#), or go to the [journal homepage](#) for more

Download details:

IP Address: 140.113.38.11

This content was downloaded on 28/04/2014 at 22:36

Please note that [terms and conditions apply](#).

Effect of Nickel Concentration on Bias Reliability and Thermal Stability of Thin-Film Transistors Fabricated by Ni-Metal-Induced Crystallization

Ming-Hui Lai, YewChung Sermon Wu, and Jung-Jie Huang^{1*}

Department of Materials Science and Engineering, National Chiao Tung University, Hsinchu 300, Taiwan, R.O.C.

¹Department of Materials Science and Engineering, Ming Dao University, Peetow, Changhua 52345, Taiwan, R.O.C.

Received July 28, 2011; revised October 3, 2011; accepted October 22, 2011; published online December 28, 2011

Ni-metal-induced crystallization (MIC) of amorphous Si (α -Si) has been employed to fabricate low-temperature polycrystalline silicon (poly-Si) thin-film transistors (TFTs). Although the high leakage current is a major issue in the performance of conventional MIC-TFTs since Ni contamination induces deep-level state traps, it can be greatly improved by using well-known technologies to reduce Ni contamination. However, for active-matrix organic light-emitting diode (AMOLED) display applications, the bias reliability and thermal stability are major concerns especially when devices are operated under a hot carrier condition and in a high-temperature environment. It will be interesting to determine how the bias reliability and thermal stability are affected by the reduction of Ni concentration. In the study, the effect of Ni concentration on bias reliability and thermal stability was investigated. We found that a device exhibited high immunity against hot-carrier stress and elevated temperatures. These findings demonstrated that reducing the Ni concentration in MIC films was also beneficial for bias reliability and thermal stability.

© 2012 The Japan Society of Applied Physics

1. Introduction

High-performance low-temperature polycrystalline silicon (LTPS) thin-film transistors (TFTs) have attracted considerable interest for use in high-resolution integrated active-matrix organic light-emitting diode (AMOLED) display, because they exhibit good electrical properties and can be used in the realization of glass substrate.¹⁾ Several technologies have been developed to reduce the crystallization temperature and time of amorphous silicon (α -Si) films. Metal-induced crystallization (MIC) is one such technology. The advantages of MIC include its low cost, good uniformity, low crystallization temperature ($\sim 500^\circ\text{C}$), and short crystallization time (0.5 to 5 h).^{2,3)} Although a high off-state current is an issue of conventional MIC-TFTs because Ni and NiSi₂ residues in the polycrystalline silicon (poly-Si) film increase the leakage current and shift the threshold voltage,^{4,5)} the situation has been greatly improved by using various techniques to reduce the Ni concentration such as the gettering method,⁶⁾ metal-induced crystallization through a cap layer (MICC),^{7,8)} and the formation of ultra thin Ni films by an atomic layer deposition (ALD) system.⁹⁾

Recently, bias reliability and thermal stability have become major concerns for AMOLED display applications, especially when devices are operated under a hot carrier condition and in a high temperature environment. It is known that hot carrier stress under high gate and high drain voltages decreases the on-current and increases the threshold voltage (V_{th}).^{10,11)} Furthermore, the other important issue is thermal stability, which increases the leakage current and shifts V_{th} with increasing in temperature.^{12,13)} Although reducing the Ni concentration is an effective way to improve the leakage current, the effect of Ni concentration on bias reliability and thermal stability is also important for AMOLED display applications. It will be interesting to determine how the reduction of Ni concentration affects the bias reliability and thermal stability of MIC-TFTs.

In this study, the effect of Ni concentration on bias reliability and thermal stability was investigated, which were reflected the behavior in the on-state and off-state regions, respectively. For comparison, the conventional MIC and

MICC methods were employed to fabricate devices with different Ni concentrations. The cap layer was formed by a chemical oxide (CF-MIC), which is simpler and cheaper than the use of SiO₂ formed by O₂ plasma. Finally, the devices were measured using a Keithley 4200 semiconductor parameter analyzer.

2. Experimental Procedure

Two kinds of poly-Si films were investigated in this study. One was an “MIC” poly-Si film fabricated by the traditional MIC method, and the other was a “CF-MIC” poly-Si film fabricated by the MICC method with a cap layer (chemical oxide) during MIC process.

A 100-nm-thick undoped α -Si layer was deposited onto a 500-nm-thick oxide-coated Si wafer by a low-pressure chemical vapor deposition (LPCVD) system. For the fabrication of chemical oxide filter MIC poly-Si films (CF-MIC), samples were dipped into a mixed solution of H₂SO₄ and H₂O₂ for 20 min to form a chemical oxide filter layer on the top of the α -Si layer. A 5-nm-thick Ni film was then deposited onto the chemical oxide/ α -Si by an e-gun evaporator. For the nickel-induced crystallization of α -Si, the heat treatment of the sample was performed at 500 °C for 1 h in N₂ atmosphere. The unreacted Ni film and chemical oxide layer were then removed by wet etching.

Typical top gated MIC poly-Si TFTs were fabricated in this study. Islands of poly-Si regions on the wafers were defined by reactive ion etching (RIE). After a cleaning process, a 100-nm-thick tetraethylorthosilicate/O₂ (TEOS) oxide layer was deposited as the gate insulator by plasma-enhanced chemical vapor deposition (PECVD). Then a 100-nm-thick poly-Si film was deposited as the gate electrode by LPCVD. After defining the gate, self-aligned 35 keV phosphorus ions were implanted at a dose of $5 \times 10^{15} \text{ cm}^{-2}$ to form the source/drain and gate. Dopant activation was performed at 600 °C for 24 h, followed by the deposition of a passivation layer and a definition of contact holes. A 500-nm-thick Al layer was then deposited by thermal evaporation and patterned as the electrode. Finally, sintering process was performed at 400 °C for 30 min in N₂ ambient.

3. Results and Discussion

As shown in Fig. 1, secondary ion mass spectroscopy (SIMS)

*E-mail address: jjhuang@mdu.edu.tw

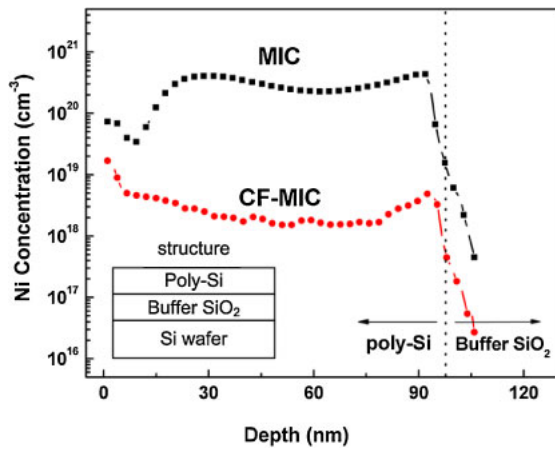


Fig. 1. (Color online) SIMS depth profiles of nickel and in the structure of poly-Si film after the MIC and CF-MIC processes.

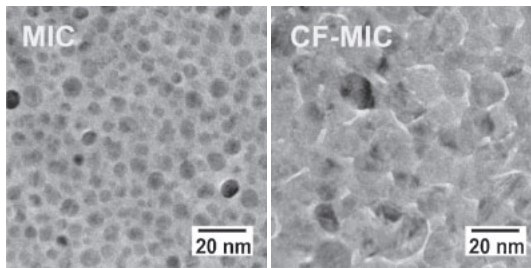


Fig. 2. Plane-view images of MIC and CF-MIC poly-Si films obtained by TEM.

depth profiles were employed to verify that the Ni concentration was reduced with the introduction of the chemical oxide filter layer. As expected, the Ni concentration in CF-MIC was much less than that in the conventional MIC, the concentrations were about 1.4×10^{18} and $2.2 \times 10^{20} \text{ cm}^{-3}$ at a depth of 50 nm, respectively. This is because the chemical oxide layer reduced the content of Ni atoms into the channel layer during MIC annealing process. Plane-view images of transmission electronic microscopy (TEM) are shown in Fig. 2. The grain diameters of MIC and CF-MIC were approximately 8–10 nm and 15–18 nm, respectively. The variation of grain size was attributed to the different Ni concentration during the MIC annealing process. The amount of nucleation sites of NiSi₂ in MIC is higher than that in CF-MIC due to the higher Ni concentration. Therefore, the grain size of MIC was less than that of CF-MIC.

Figure 3 presents the typical transfer characteristics (I_D - V_G) of the MIC and CF-MIC TFTs devices, and the key device parameters are summarized in the inset. The measurements were performed at two different drain voltages of $V_D = 0.1$ and 5 V. As can be seen, the electrical characteristics of CF-MIC TFTs were considerably superior to those of MIC TFTs, which showed a lower minimum leakage current, a higher on-state current and better field-effect mobility. The leakage current improvement was ascribed to the lower Ni concentration in the CF-MIC films. As is well known, Ni residues (Ni-related defects) serve as deep-level traps, which promote thermionic emission-dominated leakage current in the off-state region.^{14–16} In

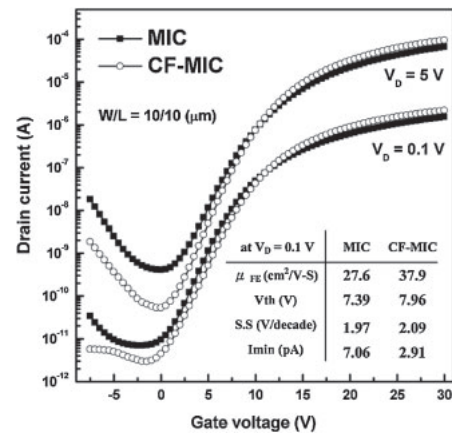


Fig. 3. Typical I_D - V_G transfer characteristics and key device parameters of conventional MIC and CF-MIC ($W/L = 10/10 \mu\text{m}$).

addition, the field-effect mobility also increased from 27.6 to $37.9 \text{ cm}^2 \text{ V}^{-1} \text{ s}^{-1}$ due to the larger grain size in CF-MIC, as shown in Fig. 2. With increasing of grain size, the effective trap state density (N_t) was decreased from 5.00×10^{12} to $4.30 \times 10^{12} \text{ cm}^{-2}$, as measured by Levinson and Proano’s method.^{17,18} Therefore, CF-MIC has higher mobility and on-current.

As above mention, reducing the Ni concentration is an effective way to improve the leakage current of MIC-TFT. However, it is interesting how the bias reliability and thermal stability are affected with the reduction of Ni concentration. According to AMOLED display applications, the bias reliability and thermal stability are considerably strict, compared with those of conventional AMLCDs. Firstly, we examined the bias reliability under hot-carrier stress at $V_{DS} = 20$ V and $V_{GS} = 20$ V for 7500 s. As respectively shown in Figs. 4 and 5, the threshold voltage and the on-current of the devices were both degraded because deep-level traps states were generated from the broken weak Si–Si and Si–H bonds.¹⁹ Compared with the conventional MIC, CF-MIC exhibits lower degradation in on-current and threshold voltage shift. The results indicate that CF-MIC possess high immunity against the hot-carrier stress with the reduction of Ni concentration. As above mention, the device with low Ni residues (CF-MIC) presented the large grain size due to the fewer nucleation sites of NiSi₂. As shown in Fig. 6, there are many weaker Si–H and Si–Si bonds at grain boundary. CF-MIC is formed with a larger grain size accompanied by fewer grain boundaries, hence leading to improved electrical reliability.^{20,21}

The other important issue of poly-Si TFTs is the thermal stability, which was examined at elevated temperatures. Figure 7 presents the I - V curves of MIC and CF-MIC, which were obtained at temperatures from 25 to 125 °C. As can be seen, the off-state curves were raised with increasing operation temperature. The threshold voltage shift and off-current as functions of temperature are summarized in Fig. 8. As shown in Fig. 8, the threshold voltage and the minimum leakage current of the devices were degraded with increasing the operation temperature. This is because nickel related donor-like defects were easy to release electrons when the operation temperature increased, thus increasing

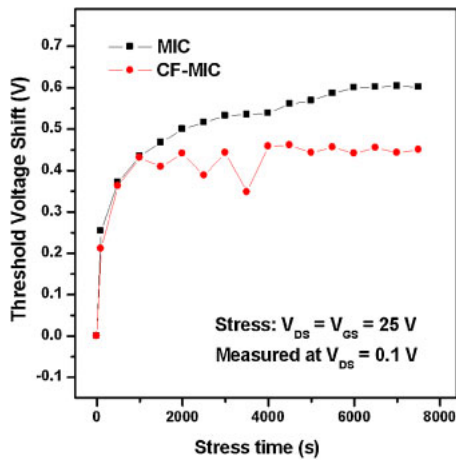


Fig. 4. (Color online) Variation of threshold voltage versus hot-carrier stress time for MIC and CF-MIC.

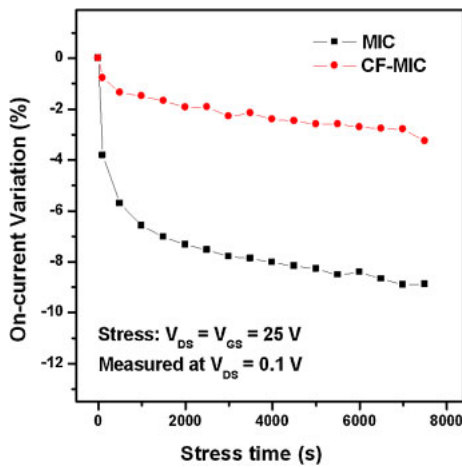


Fig. 5. (Color online) Variation of on-current versus hot-carrier stress time for MIC and CF-MIC.

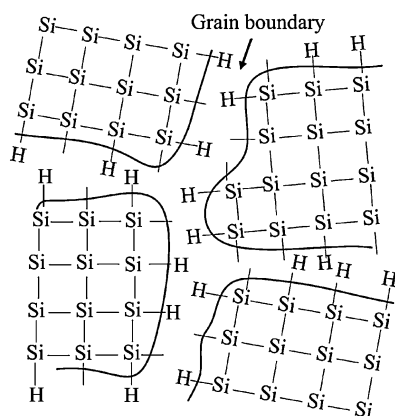


Fig. 6. Schematic showing plane-view of weak Si-H bonds and Si-Si bonds at MIC grain boundaries.

the leakage current and the negative shift of V_{th} .^{12,22)} Compared with that of MIC, the thermal stability of CF-MIC was improved by introducing a chemical oxide layer, which resulted in the reduction of Ni concentration in the devices as shown in Fig. 1. As a result, the increase in the

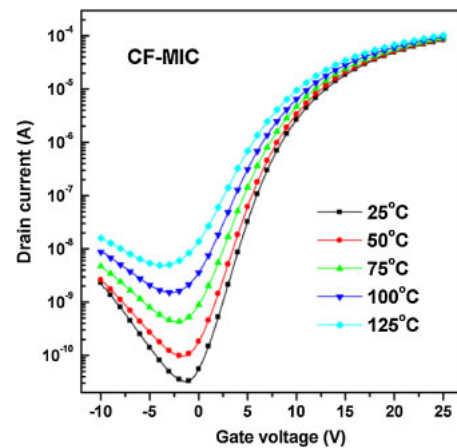
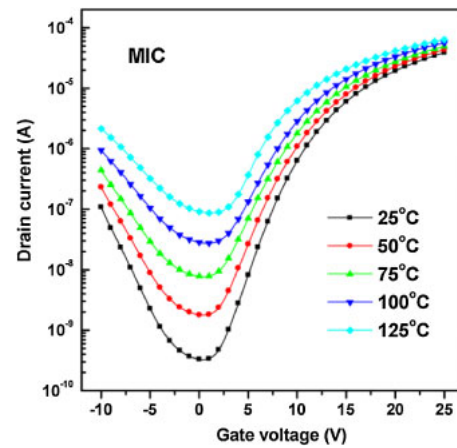


Fig. 7. (Color online) I - V curves of MIC and CF-MIC at temperatures from 25 to 125 °C.

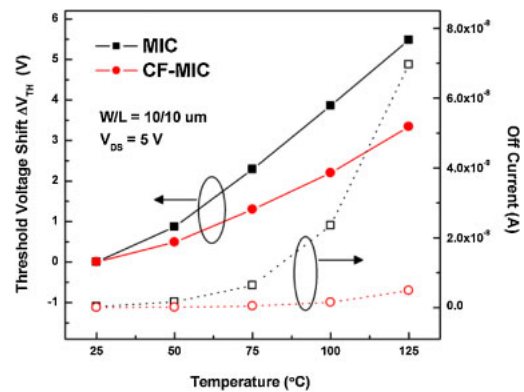


Fig. 8. (Color online) Degradations of the threshold voltage and the minimum leakage current with increasing temperature at $V_{DS} = 5$ V.

leakage current and the negative shift of V_{th} of CF-MIC were less than those of MIC. In a word, it is an appropriate course to reduce Ni concentration in an MIC-TFT, which shows not only better on-state reliability under bias stress but also better off-state stability at elevated temperatures.

4. Conclusions

It is well known that reducing the Ni concentration in MIC films is an effective way to improve leakage current. In this work, we have demonstrated that reducing the Ni concen-

tration in MIC films was also beneficial for bias reliability and thermal stability. The effects of Ni concentration effect on bias reliability and thermal stability were investigated under hot carrier stress and at elevated temperatures, respectively. As the results, the device with low Ni residues (CF-MIC) exhibited high immunity against hot-carrier stress because the fewer nucleation sites of NiSi₂ due to reduction of Ni concentration led to larger grain size and fewer weak bonds. Moreover, it was also found that reducing the Ni concentration can alleviate the degradation of threshold voltage and off current at elevated temperatures because it is easier for nickel-related donor like defects to release electrons with increasing operation temperature. These findings verify that the Ni residue reduces the performance, bias reliability, and thermal stability of MIC-TFTs.

Acknowledgements

This project was funded by Sino American Silicon Products Incorporation and the National Science Council of ROC under Grant Nos. 98-2221-E-009-041-MY3 and 99-2218-E-451-001. Technical support from the National Nano Device Laboratory, Center for Nano Science and Technology and the Nano Facility Center of the National Chiao Tung University are also acknowledged.

-
- 1) M. Stewart, R. S. Howell, L. Pires, and M. K. Hatalis: *IEEE Trans. Electron Devices* **48** (2001) 845.
 - 2) L. Pereira, H. Aguas, R. M. S. Martins, P. Vilarinho, E. Fortunato, and R. Martins: *Thin Solid Films* **451–452** (2004) 334.

- 3) C. Hayzelden and J. L. Batstone: *J. Appl. Phys.* **73** (1993) 8279.
- 4) D. Murley, N. Young, M. Trainor, and D. McCulloch: *IEEE Trans. Electron Devices* **48** (2001) 1145.
- 5) G. A. Bhat, H. S. Kwok, and M. Wong: *Solid-State Electron.* **44** (2000) 1321.
- 6) C. M. Hu, Y. C. Sermon Wu, and C. C. Lin: *IEEE Electron Device Lett.* **28** (2007) 1000.
- 7) Y. J. Chang, K. H. Kim, J. H. Oh, and J. Jang: *Electrochem. Solid-State Lett.* **7** (2004) G207.
- 8) J. H. Cheon, J. H. Bae, and J. Jang: *Electrochem. Solid-State Lett.* **10** (2007) J155.
- 9) B. S. Lim, A. Rahtu, and R. G. Gordon: *Nat. Mater.* **2** (2003) 749.
- 10) I. W. Wu, W. B. Jackson, T. Y. Huang, A. Lewis, and A. Chiang: *IEEE Electron Device Lett.* **11** (1990) 167.
- 11) F. V. Farmakis, C. A. Dimitriadis, J. Brini, G. Kamarinos, and T. E. Ivanov: *Solid-State Electron.* **43** (1999) 1259.
- 12) J. H. Kim, J. H. Choi, C. W. Kim, and J. H. Souk: *Mater. Res. Soc. Symp. Proc.* **471** (1997) 161.
- 13) C. J. Ku, Z. Duan, P. I. Reyes, Y. Lu, Y. Xu, C. L. Hsueh, and E. Garfunkel: *Appl. Phys. Lett.* **98** (2011) 123511.
- 14) C. P. Chang and Y. C. Sermon Wu: *IEEE Electron Device Lett.* **30** (2009) 130.
- 15) K. R. Olasupo and M. K. Hatalis: *IEEE Trans. Electron Devices* **43** (1996) 1218.
- 16) M. Yazaki, S. Takenaka, and H. Ohshima: *Jpn. J. Appl. Phys.* **31** (1992) 206.
- 17) R. E. Proano, R. S. Misage, and D. G. Ast: *IEEE Trans. Electron Devices* **36** (1989) 1915.
- 18) J. Levinson, G. Este, M. Rider, P. J. Scanlon, F. R. Shepherd, and W. D. Westwood: *J. Appl. Phys.* **53** (1982) 1193.
- 19) M. Hack, A. G. Lewis, and I. W. Wu: *IEEE Trans. Electron Devices* **40** (1993) 890.
- 20) Y. Uraoka, T. Hatayama, T. Fuyuki, T. Kawamura, and Y. Tsuchihashi: *Jpn. J. Appl. Phys.* **40** (2001) 2833.
- 21) A. T. Hatzopoulos, D. H. Tassis, N. A. Hastas, C. A. Dimitriadis, and G. Kamarinos: *IEEE Trans. Electron Devices* **52** (2005) 2182.
- 22) Y. Lee, S. Bae, and S. J. Fonash: *IEEE Electron Device Lett.* **26** (2005) 900.